analytical chemistry

pubs.acs.org/ac Article

Genetically Encoded Dual-Color Light-Up RNA Sensor Enabled Ratiometric Imaging of MicroRNA

Cai-Xia Dou, Chaoyang Liu, Zhan-Ming Ying,* Wanrong Dong,* Fenglin Wang,* and Jian-Hui Jiang

Cite This: *Anal. Chem.* 2021, 93, 2534−2540 Read Online

ACCESS | Metrics & More | Article Recommendations | Supporting Information

ABSTRACT: MicroRNAs (miRNAs) play essential roles in regulating gene expression and cell fate. However, it remains a great challenge to image miRNAs with high accuracy in living cells. Here, we report a novel genetically encoded dual-color light-up RNA sensor for ratiometric imaging of miRNAs using Mango as an internal reference and SRB2 as the sensor module. This genetically encoded sensor is designed by expressing a splittable fusion of the internal reference and sensor module under a single promoter. This design strategy allows synchronous expression of the two modules with negligible interference. Live cell imaging studies reveal that the genetically encoded ratiometric RNA sensor responds specifically to mir-224. Moreover, the sensor-to-Mango fluorescence ratios are linearly correlated with the concentrations of mir-224, confirming their capability of determining mir-224 concentrations in living cells. Our genetically encoded light-up RNA sensor also enables ratiometric imaging of mir-224 in different cell lines. This strategy could provide a versatile approach for ratiometric imaging of intracellular RNAs, affording powerful tools for interrogating RNA functions and abundance in living cells.

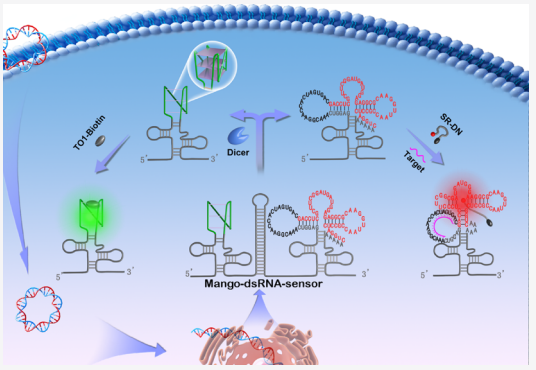

MicroRNAs (miRNAs) are short non-coding RNAs that play crucial roles in regulating gene expression and cell fate.[1,2] Methods that can provide information about their abundance, distribution, and dynamics are essential to understand their roles and functions. Nevertheless, it remains a great challenge to detect miRNAs in living cells due to their small size, intrinsic non-fluorescent nature, and low abundance.[3,4] Hybridization-based probes including molecular beacons and spherical nucleic acids have been developed to image miRNAs in living cells with high sensitivity.[5−7] However, the difficulty in delivery and susceptibility to degradation may limit their applications in determining miRNAs in living cells.[8] Genetically encoded RNA sensors that can be transcribed inside living cells could potentially overcome the issues of inefficient intracellular delivery and probe degradation.

Light-up RNA aptamers are *in vitro* selected RNA sequences that can specifically bind and activate the fluorescence of cognate non-fluorescent small molecule fluorophores.[9,10] A palette of light-up RNA aptamers including Broccoli,[11] Mango,[12] SRB2,[13] and Pepper[14] have been reported. Incorporation of the analyte-responsive motif to the light-up RNA aptamers has enabled the development of genetically encoded fluorogenic RNA sensors for imaging various analytes including small molecules,[15] proteins,[16] and RNAs[17] in living cells. However, current designs mainly rely on a single-wavelength readout that prevents them from quantitatively imaging analytes due to variations from other analyte-independent factors such as instrumental parameters and sensor concentrations. We previously reported a genetically encoded ratiometric RNA sensor for quantitative imaging mRNA, coexpressing green fluorescent protein (GFP) mRNA under a single promoter as a reference.[18] However, the requirements of translation and maturation render GFP a less-desirable reference. More recently, a genetically encoded ratiometric RNA sensor utilizing two RNA aptamers, dinitroaniline (DN) and Broccoli, was developed to quantify small molecules in bacteria.[19,20] However, the development of a genetically encoded RNA sensor based on two RNA aptamers for ratiometric imaging of RNA in mammalian cells remains unexplored.

Here, we develop a genetically encoded dual-color RNA sensor for ratiometric imaging of miRNAs in mammalian cells. We envision that the utility of two light-up RNA aptamers, one functions as an internal reference and the other functions as a sensor module, could allow the development of a genetically encoded ratiometric RNA sensor. Based on this rationale, we choose two light-up RNA aptamers, Mango and SRB2, which

Received: October 30, 2020
Accepted: January 8, 2021
Published: January 19, 2021

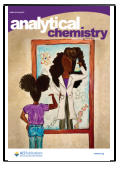

https://dx.doi.org/10.1021/acs.analchem.0c04588
Anal. Chem. 2021, 93, 2534−2540

can specifically bind and activate the fluorescence of thiazole orange biotin (TO1-Biotin)[12] and sulforhodamine B (SR)-DN,[13] respectively. Mango and SRB2 exhibit distinct spectral properties after binding with their corresponding fluorophores, facilitating dual-color imaging. A genetically encoded RNA sensor is designed by inserting a dsRNA Dicer substrate (dsRNA) that can be cleaved by endogenous Dicer enzyme[21] between the reference and the sensor module under a single promoter (Figure 1). This design allows a synchronous

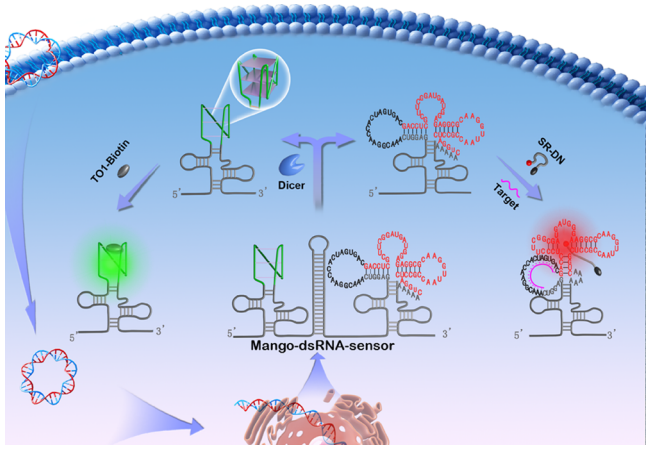

Figure 1. Scheme for the working principle of the genetically encoded dual-color light-up RNA sensor. The expressed Mango-dsRNA-sensor transcript is cleaved by Dicer to separate the reference and sensor module. The reference binds and activates the fluorescence of TO1-Biotin, whereas the sensor module hybridizes with the target miRNA and restores the correct confirmation of SRB2 with activated SR-DN fluorescence. The fluorescence ratio of SR-DN over TO1-Biotin enables ratiometric imaging of the target miRNA.

expression of the reference and the sensor module. Moreover, the dsRNA enables separation of these modules by endogenous Dicer to prevent their interaction. After expression and Dicer-mediated cleavage, the reference module can bind and activate the fluorescence of TO1-Biotin, whereas the sensor module hybridizes with the target miRNA and restores the correct confirmation of SRB2 with activated SR-DN fluorescence. The fluorescence ratios of the sensor over Mango allow ratiometric imaging of the target RNAs.

To demonstrate the concept, we choose mir-224 that is overexpressed in various cancers, especially hepatocellular carcinoma.[22,23] The sensor module is constructed by incorporating the mir-224-responsive moiety to the SR-binding loop according to our previous design strategy.[24] Fluorescence imaging reveals that the Mango-dsRNA-sensor responds specifically to mir-224, and the senor-to-Mango ratios are linearly correlated with the concentrations of mir-224 determined by quantitative reverse transcription polymerase chain reaction (qRT-PCR). Moreover, this genetically encoded dual-color RNA sensor also allows ratiometric imaging of mir-224 in different cell lines. This strategy affords a general platform for ratiometrically imaging intracellular RNAs, providing versatile tools for probing RNA functions and dynamics in living cells.

EXPERIMENTAL SECTION

Materials and Instruments. DNA oligonucleotides (HPLC) were synthesized from Sangon Biotech (Shanghai, China). RNA oligonucleotides were synthesized by TaKaRa Biotechnology (Dalian, China). A mir-224 mimic and inhibitor were obtained from RiboBio (Guangzhou, China). Oligonucleotide sequences are shown in the Supporting Information in Table S1. Restriction endonucleases and a Monarch RNA cleanup kit (50 μg) were purchased from New England Biolabs (Massachusetts, USA). Recombinant human β-actin protein was purchased from R&D Systems (Minneapolis, MN). Cell lysis buffer was purchased from Beyotime Biotechnology (Shanghai, China). HepG2, HeLa, and L-02 cells were purchased from the cell bank of Central Laboratory of Xiangya Hospital (Changsha, China). All other chemicals were of analytical grade and obtained from Sinopharm Chemical Reagent (Shanghai, China). All solutions and ultrapure water were autoclaved and treated with diethyl pyrocarbonate to avoid RNA degradation.

The fluorescence assay was performed using an F-7000 fluorescence spectrophotometer (Hitachi, Japan). A Tanon 4200SF gel imaging system (Tanon Science & Technology, China) was used to visualize the gel images. Mass spectrometry was collected on an Agilent Technologies accurate mass Q-TOF 6530 microspectrometer. Quantitative reverse transcription PCR (qRT-PCR) was carried out using an Applied Biosystems StepOnePlus PCR instrument (ABI, Foster, CA, USA). Confocal laser scanning microscopy (CLSM) images were acquired on a Nikon TI*E + A1 SI confocal laser scanning microscope (Japan) using an oil objective lens (60×).

Synthesis of TO1-Biotin Conjugate. TO1-Biotin conjugate was synthesized according to previous procedures with slight modifications.[12] Specifically, 2-(2-methylbenzo[*d*]-thiazol-3-ium-3-yl)acetate was first prepared by fluxing 2-methylbenzothiazole (1 equiv) and bromoacetic acid (1.5 equiv) in toluene for 12 h. The resulting mixture was condensed, filtrated, and washed with toluene to afford 2-(2-methylbenzo[*d*]thiazol-3-ium-3-yl)acetate with a yield of 95%. Then, 1-methylquinolinium iodide was obtained by refluxing quinoline (1 equiv) and iodomethane (2.1 equiv) in 1,4-dioxane for 1 h (50−90% yield). TO1-acetate was synthesized by stirring 1-methylquinolinium iodide (1 equiv), 2-(2-methylbenzo[d]thiazol-3-ium-3-yl)acetate (1.4 equiv), and triethylamine (3.1 equiv) in dichloromethane at room temperature overnight. The resulting mixture was precipitated with a mixture of ethanol and diethyl ether (4:1, v/v). The precipitates were filtrated and washed with water and acetone to afford TO1-acetate with a yield of 30%. Finally, TO1-Biotin was prepared by stirring a mixture composed of benzotriazole-*N*,*N*,*N*′,*N*′-tetramethyl-uronium-hexafluorophosphate (HBTU; 14 equiv), *N*,*N*-diisopropylethylamine (DIPEA; 28 equiv), TO1-acetate (1.0 equiv), and EZ-link amine-PEG-biotin (4.2 equiv) overnight at room temperature. The ultimate product, TO1-Biotin, was purified and characterized by high-resolution−electrospray ionization−mass spectrometry (HR-ESI-MS).

Fluorescence Assay. The *in vitro* transcribed RNA aptamers including 10 μM Mango, 5 μM SRB2, or 10 μM the fusion of Mango and SRB2 (M-S) were incubated with the corresponding fluorophore (10 μM TO1-Biotin or 1 μM SR-DN) in a reaction buffer (40 mM HEPES, 100 mM KCl, and 10 mM $MgCl_2$) for 30 min at 37 °C. Fluorescence spectra for TO1-Biotin were collected in the range of 515−615 nm with an excitation wavelength of 495 nm, whereas those for SR-DN were collected in the range of 565−650 nm with an excitation wavelength of 550 nm.

https://dx.doi.org/10.1021/acs.analchem.0c04588
Anal. Chem. 2021, 93, 2534−2540

To study the response of the sensor module to mir-224, a given concentration of mir-224 was incubated with the sensor module (5 μM) and 1 μM SR-DN in the reaction buffer for 30 min at 37 °C.

The selectivity study was carried out by incubating different substances including mir-224, mir-21, Let-7f, mir-222, β-actin, and L-02 cell lysates with the RNA sensor module and 1 μM SR-DN in the reaction buffer for 30 min at 37 °C. L-02 cell lysates were obtained according to the following procedures: after washing, L-02 was treated with 200 μL of cell lysis buffer for 5 min on ice. The mixture was centrifuged at 10,000g at 4 °C for 5 min, and the supernatant was collected.

Gel Imaging Assay. To test whether the RNA transcripts could bind with the corresponding fluorophores, 10 μL of 1 μM Mango, SRB2, or M-S was loaded into a well of 12% polyacrylamide gel electrophoresis (PAGE) gel. To determine whether the RNA sensor module could bind with SR-DN after reacting with mir-224, the RNA sensor module was incubated with 1 μM mir-224 at 37 °C for 30 min. The reaction mixture was loaded into a well of 12% PAGE gel. For comparison, the RNA sensor was also loaded in another well. All electrophoresis experiments were performed at a constant potential of 90 V in TBE buffer (pH 8.3) for 1 h. The PAGE gels were stained with 1 μM SR-DN or 10 μM TO1-Biotin followed by staining with a 4S GelRed nucleic acid stain. The gel was imaged with a Tanon 4200SF gel imaging system.

Vector Construction. The plasmid was constructed using pcDNA3.1(+) as a mammalian expression vector. For improving the stability of RNA, the RNA aptamers and RNA sensor were inserted into a tRNA scaffold. Overlapping PCR was utilized to obtain the DNA sequences for tRNA-scaffolded Mango-SRB2, Mango-dsRNA-SRB2, Mango-dsRNA-sensor, and Mango-dsRNA-control flanked by Hind III and PmeI cleavage sites. DNA sequences are listed in Table S1 in the Supporting Information. The PCR products were purified using a PureLink quick gel extraction kit (Thermo Scientific), according to the manufacturer's protocol. The purified products were cloned into the pcDNA3.1(+) vector under a CMV promoter via the Hind III and PmeI restriction sites to construct plasmids of Mango-SRB2, Mango-dsRNA-SRB2, Mango-dsRNA-sensor, and Mango-dsRNA-control, respectively. The resulting plasmids were confirmed by sequencing.

Cell Culture and Transfection. HepG2, HeLa, and L-02 cell lines were cultured in a 37 °C incubator with 5% CO2 using Dulbecco's modified Eagle medium (DMEM; Thermo Scientific Hyclone) added with 10% fetal bovine serum. The cells were plated on 35 mm sterilized dishes with 14 mm wells. Upon reaching a confluence of 40−60%, the cells were transfected with different plasmids using Lipofectamine 3000 (Thermo Scientific), according to the manufacturer's protocol. Typically, the cells were transfected with 500 ng of the plasmid and 2 μL of Lipofectamine 3000 in OptiMEM. The cells were then cultured in DMEM supplied with 10% FBS for 6 h before changing to a complete medium. CLSM images were obtained 24 h after transfection. To modulate the expression levels of mir-224 in HeLa cells, mir-224 mimics or inhibitors at a given dose were cotransfected with the plasmid Mango-dsRNA-sensor.

CLSM Imaging and Data Analysis. The cells in different conditions were washed with PBS three times and incubated with a DMEM medium containing 10 μM TO1-Biotin, 1 μM SR-DN conjugate, 40 mM HEPES, 100 mM KCl, and 10 mM $MgCl_2$ for 30 min at 37 °C. CLSM images were obtained after being washed with PBS three times. The fluorescence for TO1-Biotin was excited with a 488 nm laser with emission collected in the range of 495−550 nm. The fluorescence for SR-DN was excited with a 561 nm laser with the emission collected in the range of 570−640 nm. For data analysis, the average fluorescence intensity of TO1-Biotin and SR-DN was calculated by choosing 10 region of interests (ROIs) in the cytoplasm of the cells in the same field of view.

RESULTS AND DISCUSSION

Synthesis and Characterization of TO1-Biotin Conjugate. To develop a genetically encoded dual-color light-up RNA sensor, we chose Mango and SRB2 aptamers attributed to their compact sizes and distinct spectral properties of their cognate fluorophores.[12,13] We first synthesized TO1-Biotin, the ligand for Mango, and SR-DN for SRB2 was previously developed in our lab.[24] TO1-Biotin was synthesized by conjugating benzothiazole with methylquinoline, which was further derived with biotin via a linker. The compound was characterized with HR-ESI-MS (calculated for $[M + H]^+$ m/z 749.3155, found 749.3136) (Figure S1). PAGE analysis showed that Mango especially stained by the TO1-Biotin conjugate was also colored by 4S GelRed, a nucleic acid dye, confirming that TO1-Biotin could form a complex with Mango. Its cell permeability was investigated by incubating HeLa cells with varying concentrations of TO1-Biotin. Confocal laser scanning microscopy (CLSM) imaging showed negligible fluorescence for cells treated with 10 μM TO1-Biotin, which gradually increased as its concentration increased from 10 to 50 μM (Figure S2). Further, z-stacked projection analysis showed typical cytosol distribution of TO1-Biotin for cells treated with 50 μM TO1-Biotin. These results demonstrated good cell permeability of TO1-Biotin. We chose 10 μM TO1-Biotin for subsequent intracellular studies due to its low intracellular background.

Characterization of Dual-Color RNA Aptamers. The potential to construct a dual-color light-up RNA sensor using Mango and SRB2 was first explored. The transcripts of Mango, SRB2, and a fusion of Mango and SRB2 (M-S) were transcribed *in vitro*. TO1-Biotin was essentially non-emissive, but its fluorescence at ∼540 nm was dramatically increased in the presence of Mango (Figure 2A). Similarly, SR-DN exhibited negligible fluorescence but its fluorescence at ∼600 nm was remarkably enhanced in the presence of SRB2 (Figure 2B). These results revealed that Mango and SRB2 possessed distinct spectral properties, holding great potentials for dual-color fluorescence imaging. Surprisingly, there was no fluorescence enhancement for TO1-Biotin or SR-DN when incubated with the M-S transcripts, which might be due to the proximal interaction between Mango and SRB2 that hinders their correct folding. Gel electrophoresis showed consistent results that majority of M-S transcripts could not form complexes with TO1-Biotin, while M-S transcripts formed negligible complexes with SR-DN (Figure 2C,D and Figure S3). To reduce the interaction between Mango and SRB2 *in vivo*, a dsRNA Dicer substrate, which can be cleaved by abundant endogenous Dicer enzyme,[21] can be introduced to separate these two aptamers. We constructed plasmid Mango-dsRNA-SRB2 to express tRNA-scaffolded Mango-dsRNA-SRB2 under a CMV promoter (Figure S4). Gel electrophoresis analysis and positive clone sequencing confirmed its successful construction. To confirm that the transcript could be cleaved by Dicer enzyme *in vivo*, reverse transcription PCR (RT-PCR)

https://dx.doi.org/10.1021/acs.analchem.0c04588
Anal. Chem. 2021, 93, 2534−2540

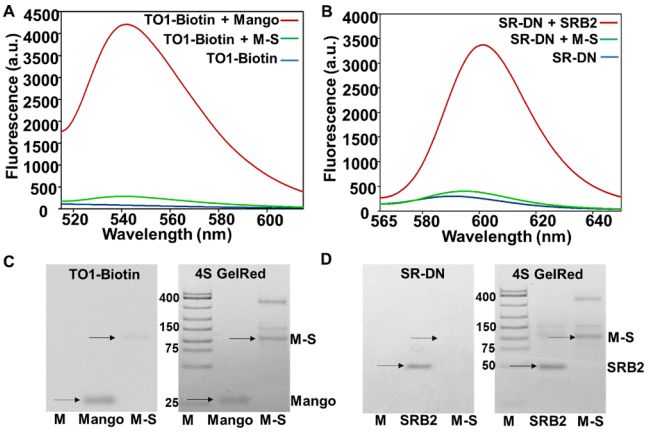

Figure 2. (A) Fluorescence spectra of TO1-Biotin in the presence of Mango and M-S transcripts (a fusion of Mango and SRB2). (B) Fluorescence spectra of SR-DN in the presence of SRB2 and M-S transcripts. (C) PAGE analysis for Mango and M-S stained by TO1-Biotin and 4S GelRed. (D) PAGE analysis for SRB2 and M-S stained by SR-DN and 4S GelRed, respectively. The lengths for Mango, SRB2, and M-S are 31, 50, and 91 nucleotides, respectively. M: DNA marker (25−500 bp).

of the total RNA extracts from HeLa cells transfected with plasmid Mango-dsRNA-SRB2 was performed using three primers designed for Mango, SRB2, and Mango-dsRNA-SRB2. Agarose gel electrophoresis analysis of the RT-PCR products revealed that the bands of Mango and SRB2 were significantly more intense than that for Mango-dsRNA-SRB2, confirming that the transcript of Mango-dsRNA-SRB2 was efficiently cleaved by intracellular Dicer enzyme (Figure S5). Further, CLSM imaging showed that HeLa cells transfected with plasmid Mango-dsRNA-SRB2 displayed strong fluorescence for TO1-Biotin and SR-DN (Figure S6). In contrast, cells transfected with a control plasmid expressing Mango-SRB2 without a Dicer substrate exhibited very dim fluorescence for TO1-Biotin and SR-DN, indicating that the separation of Mango and SRB2 was essential for fluorescence activation. In addition, z-stack images revealed that the fluorescence of TO1-Biotin and SR-DN was distributed throughout the cytoplasm (Figure S7). Together, these results demonstrated that Mango and SRB2 hold the potential for developing genetically encoded dual-color RNA sensors.

The capability of developing a reliable ratiometric sensor using Mango and SRB2 was then investigated. The SRB2-to-Mango ratios were analyzed for cells transfected with plasmid Mango-dsRNA-SRB2 at different time intervals. CLMS imaging showed that there was intense fluorescence from SRB2 and Mango 24 h post-transfection, which remained stable up to 48 h followed by a slight decrease of 60 h after transfection (Figure 3A). Time-dependent changes in the expression levels of SRB2 and Mango were confirmed by qRT-PCR analysis of the total RNA extracts from cells transfected with the plasmid Mango-dsRNA-SRB2 at different times (Figure S8). Nonetheless, further analysis showed that the average ratios of SRB2 to Mango in 10 region of interests (ROIs) in the CLSM images remained constant from 24 to 60 h after transfection (Figure 3B). Together, these results demonstrated that the SRB2-to-Mango ratios were independent of their expression levels, affording robust ratiometric imaging.

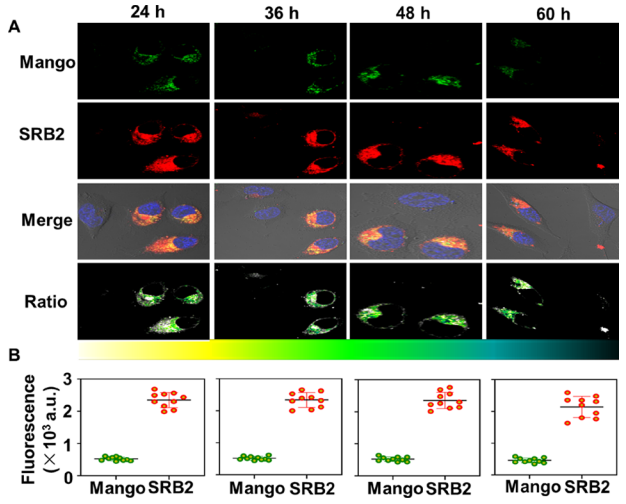

Figure 3. (A) CLSM images for HeLa cells transfected with plasmid Mango-dsRNA-SRB2 at different times. (B) Average fluorescence intensity of Mango and SRB2 in 10 ROIs.

***In Vitro* Characterization of the Sensing Module.** The feasibility of constructing an RNA sensor using SRB2 as the sensing module was first studied *in vitro*. We chose mir-224 as the target miRNA as it was overexpressed in various types of tumors including hepatocellular carcinoma.[22,23] The sensing module was constructed by incorporating the mir-224-responsive stem-loop motif to the SR binding loop of SRB2. There was negligible SRB2 fluorescence in the absence of mir-224, indicating that the integration of the mir-224-responsive motif disrupted the correct formation of SRB2 (Figure 4A). The fluorescence at 600 nm was enhanced by ∼5-fold upon incubation with 5 μM mir-224. These results demonstrated that the sensing module was responsive to mir-224. PAGE analysis gave direct evidence that SR-DN was only capable of staining the sensing module in the presence of mir-224 (Figure S9). Further investigation showed that the fluorescence for SR-

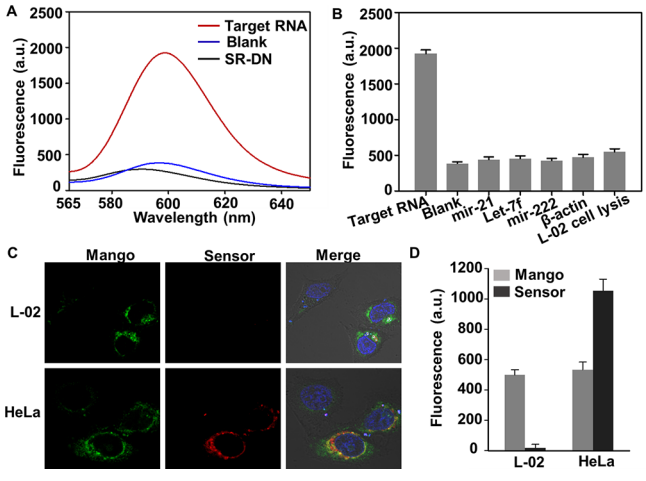

Figure 4. (A) Fluorescence responses for the sensor module: SR-DN: 1 μM SR-DN; blank: 1 μM SR-DN plus 5 μM sensor module; target RNA: 1 μM SR-DN and 5 μM sensor module plus 5 μM mir-224. (B) Selectivity study for the RNA sensor module. A fluorescence intensity at 600 nm was plotted against different substances. (C) CLSM images for cells transfected with the plasmid Mango-dsRNA-sensor for 24 h. (D) Mean fluorescence intensity of Mango and SRB2 in 10 ROIs in panel (C).

https://dx.doi.org/10.1021/acs.analchem.0c04588
Anal. Chem. 2021, 93, 2534−2540

DN increased dynamically as the concentrations of mir-224 changed from 1 nM to 5 μM (Figure S10). Additional selectivity studies revealed that the sensing module exhibited negligible fluorescence enhancement upon incubation with other intracellular components, including RNAs (mir-21, Let7f, and mir-222), proteins (β-actin), and L-02 cell lysate (Figure 4B). Together, these results demonstrated that the constructed sensing module was capable of detecting mir-224 with high sensitivity and specificity *in vitro*.

Ratiometric Imaging of MicroRNA. To develop a genetically encoded ratiometric sensor for mir-224, we constructed a plasmid expressing the reference, a Dicer substrate, and the sensing module (Mango-dsRNA-sensor) under a single CMV promoter. The capability of the Mango-dsRNA-sensor to image mir-224 was demonstrated in two cell lines, L-02 (with a negative expression of mir-224) and HeLa cells (with an overexpression of mir-224).[22,25] L-02 and HeLa cells transfected with the plasmid Mango-dsRNA-sensor exhibited bright fluorescence of TO1-Biotin in the cytosol (Figure 4C,D). By contrast, there was negligible SRB2 fluorescence for transfected L-02 cells, whereas transfected HeLa cells displayed intense SRB2 fluorescence in the cytosol. These results indicated that the sensing module was responsive to the expression levels of mir-224 in living cells, and Mango could function as a reference. Additionally, HeLa cells transfected with a plasmid expressing Mango, a Dicer substrate, and a control loop that was not complementary to mir-224 exhibited negligible fluorescence from SR-DN (Figure S11). These results demonstrated that the Mango-dsRNA-sensor responded to mir-224 in living cells with high specificity.

The capability of the Mango-dsRNA-sensor for ratiometric imaging of mir-224 was then investigated using HeLa cells treated with different concentrations of the mir-224 mimic and mir-224 inhibitor. It was known that RNA mimics can increase the levels of mature miRNAs in living cells, whereas the miRNA inhibitors can reduce the miRNA concentrations via specific hybridization.[26] CLMS images showed that there was evident and constant Mango fluorescence for cells in different conditions, suggesting that it is a reliable reference (Figure 5A). By contrast, there was varied SRB2 fluorescence for cells in different conditions. Cells treated with mir-224 mimics displayed stronger SRB2 fluorescence than the control cells without treatment, whereas cells treated with the mir-224 inhibitor showed weaker SRB2 fluorescence. Moreover, cells treated with higher concentrations of mir-224 mimics exhibited stronger SRB2 fluorescence, while those treated with higher concentrations of the mir-224 inhibitor delivered lower SRB2 fluorescence. Further ratiometric images using the sensor-to-Mango fluorescence ratios showed a distinct color shift for cells under different treatments. Moreover, the average of sensor-to-Mango fluorescence ratios in 10 ROIs was linearly correlated with the relative concentrations of mir-224, as determined by qRT-PCR using U6 as a reference RNA (Figure 5B,C). Collectively, these results demonstrated that the Mango-dsRNA-sensor was capable of ratiometrically imaging mir-224 in living cells.

The Mango-dsRNA-sensor was further utilized to image mir-224 in different cells. Three cell lines, HepG2, HeLa, and L-02, with different expression levels of mir-224 were chosen. There was bright fluorescence from Mango for all the cells, whereas the fluorescence for SRB2 varied in different cells (Figure 6A). HepG2 cells displayed the most intense SRB2 fluorescence, while HeLa cells showed intermediate SRB2

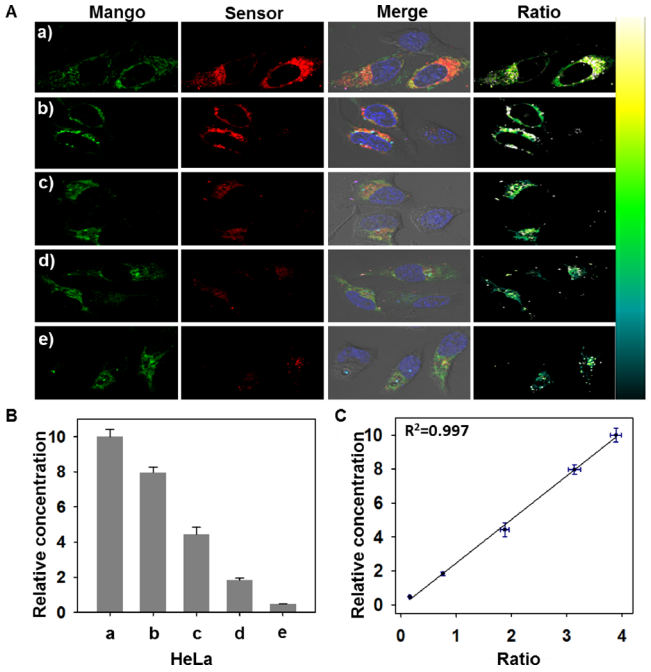

Figure 5. (A) CLSM images of HeLa cells transfected with the plasmid Mango-dsRNA-sensor under different conditions. (a) 250 nM mir-224 mimic. (b) 50 nM mir-224 mimic. (c) Plasmid only. (d) 50 nM mir-224 inhibitor. (e) 250 nM mir-224 inhibitor. (B) Relative concentrations of mir-224 obtained from qRT-PCR under different conditions. (C) Liner correlation between mir-224 expression levels and average sensor-to-Mango ratios in 10 ROIs.

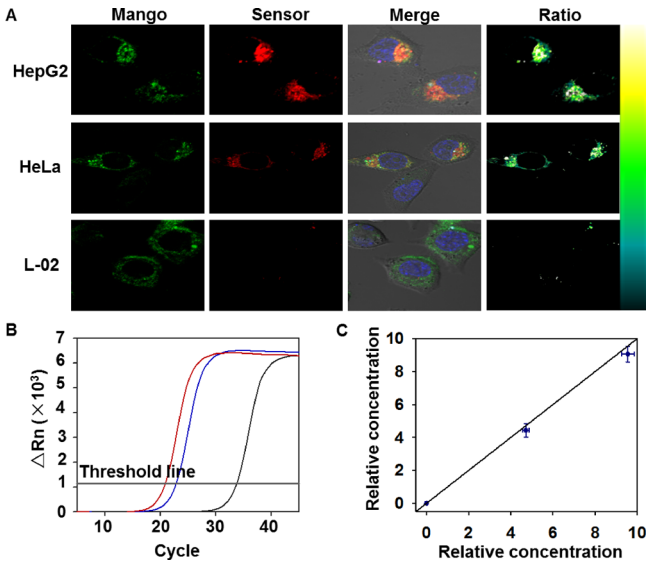

Figure 6. (A) CLSM images of different cell lines transfected with the plasmid Mango-dsRNA-sensor. (B) qRT-PCR analysis of mir-224 for different cell lines. The red, blue, and black lines denote the cell line of HepG2, HeLa, and L-02, respectively. (C) Correlation of relative concentrations calculated based on sensor-to-Mango ratios in panel (A) using the calibration curve in Figure 5C (x axis) and those determined by qRT-PCR analysis in panel (B) using U6 as a reference (y axis).

fluorescence. By contrast, the SRB2 fluorescence in L-02 was very dim. These results demonstrated that HepG2, HeLa, and L-02 cells had decreased mir-224 levels, which were consistent with the previous studies[22,25] and qRT-PCR results (Figure

https://dx.doi.org/10.1021/acs.analchem.0c04588
Anal. Chem. 2021, 93, 2534−2540

6B). The relative expression levels of mir-224 in different cell lines were calculated based on the calibration curve in Figure 5C using the average sensor-to-Mango ratios and determined based on the qRT-PCR results using U6 as the internal reference (Figure S12). It was revealed that the relative concentrations of mir-224 determined by utilizing the calibration curve in Figure 5C are highly correlated with those obtained from qRT-PCR (Figure 6C). These results further demonstrated that our genetically encoded ratiometric sensor could accurately image the levels of mir-244 in different cells.

CONCLUSIONS

We developed a novel genetically encoded dual-color light-up RNA sensor using Mango as the reference and SRB2 as the sensing module for ratiometric imaging of miRNA in living mammalian cells. We demonstrated that a direct fusion of SRB2 and Mango failed to show fluorescence enhancement for both RNA aptamers *in vitro* and in living cells. Splitting of the RNA aptamers by integration of a Dicer substrate restored the fluorescence for both SRB2 and Mango. We demonstrated that the fluorescence of SRB2-to-Mango ratios remained constant at different times upon transfection, affording a reliable ratiometric imaging platform. This genetically encoded sensor was successfully utilized to ratiometrically imaging mir-224 in tumor cells under different treatments. It was revealed that the sensor-to-Mango fluorescence ratios were linearly correlated with the concentrations of mir-224 obtained from qRT-PCR. The developed sensor also allowed ratiometric imaging of mir-224 in different cell lines. Our design may afford a robust platform for developing genetically encoded light-up RNA sensors for quantitative imaging of RNAs in living cells.

ASSOCIATED CONTENT

Supporting Information

The Supporting Information is available free of charge at https://pubs.acs.org/doi/10.1021/acs.analchem.0c04588.

Experimental method, DNA and RNA sequence, scheme of plasmid expression, characterization of TO1-Biotin, plasmid map, gel electrophoresis analysis, fluorescence spectra, CLSM images, and additional data (PDF)

AUTHOR INFORMATION

Corresponding Authors

Zhan-Ming Ying − *State Key Laboratory of Chemo/Bio-Sensing and Chemometrics, College of Chemistry and Chemical Engineering, Hunan University, Changsha, Hunan 410082, China*; Email: zmying@hnu.edu.cn

Wanrong Dong − *State Key Laboratory of Chemo/Bio-Sensing and Chemometrics, College of Chemistry and Chemical Engineering, Hunan University, Changsha, Hunan 410082, China*; orcid.org/0000-0002-6541-2853; Email: wanrongdong@hnu.edu.cn

Fenglin Wang − *State Key Laboratory of Chemo/Bio-Sensing and Chemometrics, College of Chemistry and Chemical Engineering, Hunan University, Changsha, Hunan 410082, China*; orcid.org/0000-0002-5872-2693; Email: fengliw@hnu.edu.cn; Fax: +86-731-88821916

Authors

Cai-Xia Dou − *State Key Laboratory of Chemo/Bio-Sensing and Chemometrics, College of Chemistry and Chemical Engineering, Hunan University, Changsha, Hunan 410082, China*

Chaoyang Liu − *State Key Laboratory of Chemo/Bio-Sensing and Chemometrics, College of Chemistry and Chemical Engineering, Hunan University, Changsha, Hunan 410082, China*

Jian-Hui Jiang − *State Key Laboratory of Chemo/Bio-Sensing and Chemometrics, College of Chemistry and Chemical Engineering, Hunan University, Changsha, Hunan 410082, China*; orcid.org/0000-0003-1594-4023

Complete contact information is available at: https://pubs.acs.org/10.1021/acs.analchem.0c04588

Notes

The authors declare no competing financial interest.

ACKNOWLEDGMENTS

This work was financially supported by the National Natural Science Foundation of China (21904034, 21806033, 21974041, and 91753107) and the Natural Science Foundation of Hunan Province (2017JJ3027).

REFERENCES

(1) Bartel, D. P. *Cell* **2004**, *116*, 281−297.
(2) Vidigal, J. A.; Ventura, A. *Trends Cell Biol.* **2015**, *25*, 137−147.
(3) Baker, M. *Nat. Methods* **2012**, *9*, 787−790.
(4) Qing, Z.; Xu, J.; Hu, J.; Zheng, J.; He, L.; Zou, Z.; Yang, S.; Tan, W.; Yang, R. *Angew. Chem., Int. Ed.* **2019**, *58*, 11574−11585.
(5) Xue, C.; Zhang, S.; Li, C.; Yu, X.; Ouyang, C.; Lu, Y.; Wu, Z. S. *Anal. Chem.* **2019**, *91*, 15678−15685.
(6) Li, L.; Feng, J.; Liu, H.; Li, Q.; Tong, L.; Tang, B. *Chem. Sci.* **2016**, *7*, 1940−1945.
(7) Rouge, J. L.; Sita, T. L.; Hao, L.; Kouri, F. M.; Briley, W. E.; Stegh, A. H.; Mirkin, C. A. *J. Am. Chem. Soc.* **2015**, *137*, 10528−10531.
(8) Bao, G.; Rhee, W. J.; Tsourkas, A. *Annu. Rev. Biomed. Eng.* **2009**, *11*, 25−47.
(9) Paige, J. S.; Wu, K. Y.; Jaffrey, S. R. *Science* **2011**, *333*, 642−646.
(10) Neubacher, S.; Hennig, S. *Angew. Chem., Int. Ed.* **2019**, *58*, 1266−1279.
(11) Filonov, G. S.; Moon, J. D.; Svensen, N.; Jaffrey, S. R. *J. Am. Chem. Soc.* **2014**, *136*, 16299−16308.
(12) Dolgosheina, E. V.; Jeng, S. C. Y.; Panchapakesan, S. S. S.; Cojocaru, R.; Chen, P. S. K.; Wilson, P. D.; Hawkins, N.; Wiggins, P. A.; Unrau, P. J. *ACS Chem. Biol.* **2014**, *9*, 2412−2420.
(13) Sunbul, M.; Jäschke, A. *Angew. Chem., Int. Ed.* **2013**, *52*, 13401−13404.
(14) Chen, X.; Zhang, D.; Su, N.; Bao, B.; Xie, X.; Zuo, F.; Yang, L.; Wang, H.; Jiang, L.; Lin, Q.; Fang, M.; Li, N.; Hua, X.; Chen, Z.; Bao, C.; Xu, J.; Du, W.; Zhang, L.; Zhao, Y.; Zhu, L.; Loscalzo, J.; Yang, Y. *Nat. Biotechnol.* **2019**, *37*, 1287−1293.
(15) Su, Y.; Hickey, S. F.; Keyser, S. G. L.; Hammond, M. C. *J. Am. Chem. Soc.* **2016**, *138*, 7040−7047.
(16) Song, W.; Strack, R. L.; Jaffrey, S. R. *Nat. Methods* **2013**, *10*, 873−875.
(17) Cawte, A. D.; Unrau, P. J.; Rueda, D. S. *Nat. Commun.* **2020**, *11*, 1283.
(18) Ying, Z. M.; Yuan, Y. Y.; Tu, B.; Tang, L. J.; Yu, R. Q.; Jiang, J. H. *Chem. Sci.* **2019**, *10*, 4828−4833.
(19) Wu, R.; Karunanayake Mudiyanselage, A. P. K. K.; Shafiei, F.; Zhao, B.; Bagheri, Y.; Yu, Q.; McAuliffe, K.; Ren, K.; You, M. *Angew. Chem., Int. Ed.* **2019**, *58*, 18271−18275.
(20) Wu, R.; Karunanayake Mudiyanselage, A. P. K. K.; Ren, K.; Sun, Z.; Tian, Q.; Zhao, B.; Bagheri, Y.; Lutati, D.; Keshri, P.; You, M. *ACS Appl. Bio Mater.* **2020**, *3*, 2633−2642.

(21) Sinha, N. K.; Iwasa, J.; Shen, P. S.; Bass, B. L. *Science* **2018**, *359*, 329−334.
(22) Wang, Y.; Lee, A. T. C.; Ma, J. Z. I.; Wang, J.; Ren, J.; Yang, Y.; Tantoso, E.; Li, K.-B.; Ooi, L. L. P. J.; Tan, P.; Lee, C. G. L. *J. Biol. Chem.* **2008**, *283*, 13205−13215.
(23) Murakami, Y.; Yasuda, T.; Saigo, K.; Urashima, T.; Toyoda, H.; Okanoue, T.; Shimotohno, K. *Oncogene* **2006**, *25*, 2537−2545.
(24) Ying, Z.-M.; Wu, Z.; Tu, B.; Tan, W.; Jiang, J.-H. *J. Am. Chem. Soc.* **2017**, *139*, 9779−9782.
(25) Liao, X.; Wang, Q.; Ju, H. *Chem. Commun.* **2014**, *50*, 13604−13607.
(26) Li, J.; Tan, S.; Kooger, R.; Zhang, C.; Zhang, Y. *Chem. Soc. Rev.* **2014**, *43*, 506−517.

https://dx.doi.org/10.1021/acs.analchem.0c04588
Anal. Chem. 2021, 93, 2534−2540